Food Hydrocolloids 154 (2024) 110153

Contents lists available at ScienceDirect

Food Hydrocolloids

journal homepage: www.elsevier.com/locate/foodhyd

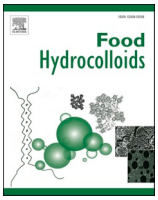

The ice recrystallization inhibition activity of wheat glutenin hydrolysates and effect of salt on their activity

Yuan Yuan, Vermont P. Dia *, Tong Wang **

Department of Food Science, University of Tennessee Institute of Agriculture, 2510 River Dr., Knoxville, TN, 37996, USA

ARTICLE INFO

Keywords:
Wheat glutenin hydrolysates
Ice recrystallization activity
Salt concentration
Ionic strength
Protein secondary structure

ABSTRACT

This study aimed to investigate the antifreeze activity of wheat glutenin hydrolysates produced by Alcalase and trypsin at varying degrees of hydrolysis. The influence of salt concentrations in two dispersing media, phosphate-buffered saline (PBS) and NaCl solution, and the types of cations, NaCl and $CaCl_2$, on hydrolysates was further analyzed. The results revealed a consistently higher ice recrystallization inhibition (IRI) activity for all hydrolysates dispersed in 0.1 x PBS than in 1 x PBS. Interestingly, glutenin hydrolysates exhibited better IRI activity in $CaCl_2$ than in NaCl solution under the same ionic strength. Furthermore, trypsin-derived hydrolysates (with a molar mass about 10 kDa) consistently had better IRI activity than those produced by Alcalase (with a molar mass less than 1 kDa), regardless of the dispersing media. The observed increase in IRI activity was associated with alterations in the secondary structure, characterized by a higher α-helix and lower β-turns content. This suggests that structural rigidity of the molecules plays a significant role in enhancing the antifreeze activity of peptides. Additionally, the scores plot of the partial least-squares discriminant analysis model indicates that salt concentration had a more significant impact than salt type on the IRI activity of glutenin hydrolysates. In conclusion, our findings provide insights into the factors influencing the IRI activity of protein hydrolysates.

1. Introduction

Antifreeze peptides have long been studied for their potential applications in frozen food, as they can control the formation and growth of ice crystals (Biggs et al., 2019). Although the mechanism of these peptides is still elusive, some characteristics have been identified. Firstly, hydrophobic groups were reported to be associated with stronger antifreeze activity. For example, antifreeze glycoproteins can bind to ice through their hydrophobic methyl groups (Mochizuki & Molinero, 2018). Secondly, many antifreeze peptides contain proline residues (Damodaran & Wang, 2017; Yang et al., 2022). Computational modeling also showed that tetrapeptide with proline residues is more effective in retarding crystal growth compared to glycine (Kim, Damodaran, & Yethiraj, 2009). Additionally, peptides with acidic amino acid residues like glutamic acid often exhibit superior antifreeze activity compared to peptides from other sources (Luo et al., 2023; Yang et al., 2022).

Wheat flour typically contains 10–15 % protein (Wieser, Koehler, & Scherf, 2022), with approximately 35 % of its amino acids being hydrophobic and proline-rich (Sivam, Sun-Waterhouse, Quek, & Perera, 2010). However, wheat protein is a complex mixture, and it is classified into four groups, namely albumin, globulin, gliadin, and glutenin, according to their solubilities in various solvents (Lookhart, 1995). The first two fractions are non-gluten proteins, constituting around 15–20 % of total wheat protein, while the latter two fractions, gliadin and glutenin, are classified as gluten proteins, accounting for approximately 80–85 % of the total wheat protein (Thewissen, Celus, Brijs, & Delcour, 2011). These fractions exhibit distinct molecular size, amino acid composition, and functionality. Gluten hydrolysates have demonstrated cryoprotective properties on frozen dough (Zhang et al., 2022). However, the specific proteins or molecular characteristics of the protein hydrolysates responsible for this activity have not been elucidated in previous studies. Given that glutenin, the largest component of gluten (Urade, Sato, & Sugiyama, 2018), is hydrophobic and rich in proline and glutamic acid, the use of proteases to generate hydrolysates as antifreeze agents becomes pertinent. These hydrolysates, enriched with glutamic acid and proline residues, hold the potential to inhibit ice crystal growth originating from a common food protein.

The standard splat assay is a commonly used method for detecting ice

* Corresponding author.
** Corresponding author.
E-mail addresses: vdia@utk.edu (V.P. Dia), twang46@utk.edu (T. Wang).

https://doi.org/10.1016/j.foodhyd.2024.110153
Received 5 February 2024; Received in revised form 25 March 2024; Accepted 30 April 2024
Available online 30 April 2024

recrystallization inhibition (IRI) activity (Delesky & Srubar, 2022). Typically, this assay is conducted in the presence of >2 mM NaCl or 1 x phosphate-buffered saline (PBS), which contains NaCl, KCl, Na_2HPO_4, and KH_2PO_4, to prevent false positives results (Voets, 2017). Despite its frequent use, few studies have investigated how different salt types and concentrations in dispersing media influence the IRI activity of peptides. In a study by Leiter et al. (2016), the addition of 30 mM NaCl showed a synergetic effect with antifreeze protein (AFP) III under a 49 % sucrose solution condition. However, they did not explain the reason, and the sucrose concentration may be too high to accurately describe the effect of salt. Moreover, the choice of salts in the dispersing media can also influence the IRI effects of peptides. For example, Suris-Valls and Voets (2019) compared the ice crystal size of antifreeze glycoprotein $(AFGP)_{1\text{-}5}$ and type III AFP in sodium nitrate, sodium chloride, sodium borate, sodium phosphate, and sodium citrate buffers and discovered that the citrate buffer consistently led to higher IRI activity for both proteins. In addition, certain Ca^{2+} ions have an additional impact on the antifreeze activity of proteins. For example, type II AFP exhibits Ca^{2+} dependent activity (Arai, Nishimiya, Ohyama, Kondo, & Tsuda, 2019).

Therefore, the choice of salts in dispersing media is not only crucial for IRI activity but also has a significant impact on the conformation of proteins. Salt at a low concentration stabilizes the proteins and hence impacts their conformation (Tsumoto, Ejima, Senczuk, Kita, & Arakawa, 2007). Moreover, different ions can influence the conformation of peptides, as observed in the orientation of Ca^{2+} binding residues in type II AFP in the presence of Ca^{2+} (Arai et al., 2019), which affects its ice-binding activity. The antifreeze activity of proteins is known to correlate with their rigid conformation (Patel & Graether, 2010). AFPs and AFGPs, known for their high IRI activity, possess rigid structures primarily due to α-helix and polyproline II helix, respectively (Mochizuki et al., 2018; Nishimiya et al., 2006; Sicheri & Yang, 1996). This characteristic has been used in the synthesis of triplex metallohelices, demonstrating potent IRI activity that emphasizes the importance of rigid helix structures on effective ice interaction (Mitchell et al., 2017). In addition to IRI activity, peptides with a high α-helix structure also tend to exhibit higher thermal hysteresis activity (Rojas et al., 2022), which can related to antifreeze activity. Furthermore, antifreeze peptides from shrimp (Zhu, Zheng, & Dai, 2022), silver carp (Wang et al., 2021), *Taki Fugu obscurus* skin (Yang et al., 2022), and Antarctic yeast protein (Shah et al., 2012) are all characterized by an α-helix structure. Peptides with an α-helix may have a more stable conformation, which is related to antifreeze activity (Zhang et al., 2018).

Based on these findings, our hypothesis is that wheat glutenin hydrolysates may exhibit potent IRI activity due to their unique amino acid profile, and the strength of this activity may be influenced by molecular size, secondary structure, and condition of dispersing media that modify their conformations. The objective of this study is to evaluate the IRI activity of wheat glutenin hydrolysates under different salt concentrations (0.1× PBS and 1 x PBS) and salt solutions (NaCl and $CaCl_2$ solution) and correlate this to their secondary structure.

2. Materials and methods

2.1. Materials

Wheat flour (Bob's Red Mill) was purchased from the local grocery store. The Alcalase from *Bacillus licheniformis* (3.03 U/mL) was purchased from EMD Millipore Corp (Massachusetts, USA), and trypsin from porcine pancreas was purchased from Sigma-Aldrich company (Missouri, USA).

2.2. Glutenin hydrolysates preparation

The extraction of glutenin from wheat flour followed the Osborne fractionation method as outlined by Lookhart and Scott (1995) with a slight modification. In brief, 100 g of wheat flour underwent sequential extractions with DI water, 0.5 M NaCl, and 70% ethanol to eliminate albumin, globulin, and gliadin. Subsequently, the residual material was initially combined with 400 mL of 50% 2-propanol containing 1% dithiothreitol to disrupt disulfide bonds. After centrifugation at 5388 rpm (equivalent to 5000×*g*) for 10 min, the precipitate was extracted with 400 mL of 0.05 M NaOH solution for three times. The extracted glutenin supernatant was dialyzed (3.5 kDa) and subsequently lyophilized. Given that glutenin is not soluble in aqueous solutions, it was subjected to hydrolysis by Alcalase and trypsin independently. For the Alcalase hydrolysis, glutenin powder was mixed with DI water (at a 5 % concentration, w/w), and the pH was adjusted to 8.0 using 0.2 M NaOH. The enzyme-to-substrate ratio was set at 0.176 Anson units per gram of the powder. The mixture was then incubated at 55 °C for 5, 15, and 30 min. In the case of trypsin hydrolysis, the enzyme was introduced at a concentration of 180 units per gram of glutenin powder, and the pH was adjusted to 8.0 using 0.5 M NaOH. The hydrolysis times were 1, 2, 3, and 4 h. After completion of the hydrolysis process, all samples were boiled for 10 min to deactivate the enzyme. Subsequently, all samples were centrifuged for 5 min at 5388 rpm (equivalent to 5000×*g*), and the resulting supernatant was freeze-dried for further characterization and analysis. The yield of glutenin hydrolysates was calculated by the mass of freeze dried supernatant relative to the mass of initial glutenin powder.

2.3. Amino acid composition and protein content determination

The method used was that of Akhlaghi et al (2015) with slight modifications. Samples (1 mg/mL) were hydrolyzed by 6 M HCl at 150 °C for 30 min. After hydrolysis, the samples were dried under vacuum at 50–60 °C overnight, then sample buffer (50 mM $NaHCO_3$, pH = 8.4) was used to dissolve and dilute the sample. Subsequently, 200 μL of the diluted samples were mixed with 300 μL of 4 mM dabsyl chloride and vortexed for 30 s. The mixture was then heated at 70 °C for 20 min. Next, 500 μL of diluent solution, consisting of a mixture of 50 mM sodium phosphate buffer (pH = 7.0) and HPLC-grade ethanol was added. The resulting solutions were filtered by a 0.45 μm Nylon filter for HPLC analysis. HPLC analysis was performed using a Zorbax Eclipse Plus C18 column under the following conditions: 10 μL of injection volume, a flow rate of 1 mL/min, and a column temperature of 40 °C. The UV–Vis detector wavelength was at 436 nm. Sodium acetate buffer (25 mM, pH = 6.5) containing 4 % dimethylformamide was used as mobile phase A, and acetonitrile was used as mobile phase B. A gradient elution program was employed with the following time (min)/percentage B values: 0/15, 20/40, 32/70, 34/70, 35/15, 45/15. To construct the standard curve, an amino acid (AA) standard mixture (Sigma, AA-S-18) containing 17 AA standards was utilized. The standards were prepared by diluting the standard mixture to concentrations of 1.56, 3.13, 6.25, 12.50, and 25.00 nmol of all amino acid standards in tubes using the sample buffer. The protein content determination was calculated by adding up the weights of all amino acids.

2.4. Phenol-sulfuric acid method for total carbohydrates assay

The method of Nielsen (2017) was used with slight modifications. Briefly, 1 mL sample (1 mg/mL) was mixed with 25 μL of 80 % phenol solution and 2.5 mL of concentrated sulfuric acid, and left to stand for 10 min. After cooling to room temperature, the absorbance was measured at 490 nm. Glucose was used as standard for qualification.

2.5. Size exclusion chromatography for average molecular weight determination

The molecular weight of glutenin and its corresponding hydrolysates was analyzed by a BioSep-SEC-s2000 column (Phenomenex, Torrance, CA, USA), with the mobile phase comprised of a 45:55 (v/v) mixture of acetonitrile and HPLC-grade water with 0.05 % trifluoroacetic acid. The

molecular weight distribution was determined by comparing the elution profile with a mixture of protein standards with known molecular weights (M_w) detected at 214 nm. Retention times and the logarithm of M_w for standards (albumin, aprotinin, bradykinin acetate, bradykinin fragment 1–5, glutathione, and glycine) were employed to construct a linear standard curve ($R^2 = 0.992$). The established standard curve equation was then utilized to calculate the M_w of each peak in the chromatogram. The average M_w was computed based on the percentage contribution of each peak, as determined by the area under the curve.

2.6. O-pthaldialdehyde (OPA) method for determining relative degree of hydrolysis

The degree of hydrolysis (DH) of hydrolysates was analyzed following a previous study (Spellman, McEvoy, O'Cuinn, & FitzGerald, 2003) with minor modifications. The fresh OPA reagent was prepared by combining 25 mL of 100 mM borax, 2.5 mL of a 20 % SDS solution, a solution containing 40 mg of OPA dissolved in 1 mL of methanol, 100 μL of β-mercaptoethanol, and DI water, adjusting the solution to a final volume of 50 mL. The hydrolysates were dissolved in 1x PBS solution at a concentration of 1 mg/mL. Ten μL of each sample was placed in a well in a 96-well plate and filled with 200 μL of the freshly prepared OPA reagent. A fully hydrolyzed glutenin was prepared by dissolving it in 6 M HCl at 110 °C overnight at a concentration of 1 mg/mL. Absorbance was read using a Cambrex ELx808 Microplate Reader at 340 nm after incubating for 5 min. The DH values were calculated using the following formula:

$$DH\ \% = \frac{absorbance\ of\ hydrolysates}{absorbance\ of\ fully\ hydrolyzed\ glutenin} \times 100$$

2.7. Splat assay for IRI activity

The splat assay was carried out as previously reported (Knight, Hallett, & DeVries, 1988) and calculated as we previously reported (Yuan, Fomich, Dia, & Wang, 2023), with sample solutions containing varying concentrations (1–40 mg/mL) prepared by dissolving in 1x PBS, 0.1 x PBS, 10 mM NaCl, 10 mM CaCl2, and 30 mM NaCl. Samples were prepared in duplicate, and each sample was analyzed twice in independent slides. The slide was annealed at −8 °C for 30 min, and three pictures were captured from each slide, from which the Feret's maximum diameter was averaged by ImageJ software (Saad, Fomich, Dia, & Wang, 2023). The relative ice recrystallization inhibition activity was shown as ICS, which was calculated by dividing the average ice crystal size of the treated sample by that of the control sample, which contained the same concentration of polyethylene glycol in the same dispersing media. ICS was chosen as the indicator rather than the absolute ice crystal size because ICS provides a relative measure of the effectiveness of the hydrolysates in inhibiting ice crystal growth as previously reported (Bachtiger, Congdon, Stubbs, Gibson, & Sosso, 2021).

2.8. Fourier transform infrared (FTIR) for secondary structure analysis of hydrolysates

The secondary structure of hydrolysates was analyzed by FTIR using Spectrum Two FT-IR Spectrometer (PerkinElmer Inc., Waltham, MA, US). Hydrolysates were prepared in 1 x PBS, 0.1 x PBS, 10 mM NaCl, 10 mM $CaCl_2$, and 30 mM NaCl solution at a concentration of 40 mg/mL. The spectra were recorded with 32 scans in the region between 1800 and 1500 cm^{-1} range with a resolution of 4 cm^{-1} and data were analyzed using PerkinElmer Spectrum IR software (Sadat & Joye, 2020). The amide I band (1600–1700 cm^{-1}) in each spectrum was interpreted by Origin 2021 Pro software to determine peptide's secondary structure. The band regions at 1610-1640 cm^{-1} and 1670-1690 cm^{-1} were assigned as β-sheet, and the random coil and α-helix ranges were 1640–1650 cm^{-1} and 1650-1660 cm^{-1}, respectively. The peaks at 1660-1670 cm^{-1} and 1690-1700 cm^{-1} were also reported to result from β-turn (Yuan et al., 2023). FTIR was used instead of circular dichroism as FTIR can directly analyze proteins in complex food matrices without the need for prior protein extraction (Sadat, Corradini, & Joye, 2019). Our sample contains 16.9% carbohydrates, hence circular dichroism is not ideal as this will require protein extraction prior to analysis (Sadat & Joye, 2020).

Table 1
Yield and property of hydrolysates of wheat glutenin made by two proteases.

Protease	Hydrolysis time (min)	DH (%)	Average M_w (KDa)	Yield (%) [a]	ICS (%) [b]
Alcalase	5	15.2 ± 1.5[b]	0.8 ± 0.1 [a]	63.8 ± 4.0	88.4 ± 2.6
	15	26.9 ± 3.5[a]	0.6 ± 0.1[ab]	66.1 ± 0.9	83.7 ± 8.4
	30	31.3 ± 4.1[a]	0.5 ± 0.0 [b]	71.8 ± 6.5	84.5 ± 5.2
Trypsin	60	12.3 ± 1.4[b]	15.1 ± 1.6 [a]	37.9 ± 1.5 [c]	71.1 ± 1.3[bc]
	120	15.4 ± 1.8[b]	13.7 ± 0.1[ab]	45.7 ± 0.8 [b]	77.0 ± 3.6 [a]
	180	15.7 ± 2.0[b]	9.8 ± 1.0 [b]	46.5 ± 0.2[ab]	68.3 ± 3.4 [c]
	240	21.8 ± 3.4[a]	9.8 ± 1.6 [b]	50.9 ± 1.7 [a]	73.8 ± 1.4[ab]

Different lowercase letter in the same column and enzyme indicates significant differences among means ($P < 0.05$).

[a] The mass balance was relative to the starting dry glutenin powder obtained by Osborne fractionation.

[b] The IRI activity was expressed as the average ice crystal size (ICS) relative to the same concentration (40 mg/mL) of PEG negative control in 1 x PBS, with lower values representing higher activity.

2.9. Statistical analysis

The statistical analysis was performed based on the results of two independent trials of the experiment, and each trial was repeated 3 times. All data were reported as average ± standard deviation and processed by Excel 2016, and SPSS 22.0, and figures were prepared using Origin 2021 Pro. Principal component analysis (PCA) was created using Origin Pro apps, and partial least-squares discriminant analysis (PLS-DA) score plots were derived with the SIMCA-P software (Version 14.1, Umetrics AB, Umea, Sweden). The statistical significance of the data was determined using one-way analysis of variance (ANOVA) followed by the Duncan test, and the significance was established at $P < 0.05$.

3. Results and discussion

3.1. Effect of enzyme type and hydrolysis time on peptides' size and IRI activity

After Osborne fractionation, the yield of glutenin is 7.6 % based on dry wheat flour powder. The protein content of the isolated glutenin accounted for 83.9 %, with 16.9 % carbohydrates. This result indicates that the extracted glutenin samples contain sufficient protein for further analysis. However, glutenin is not water-soluble, so proteases (Alcalase and trypsin) were used to increase its solubility. As the hydrolysis time increased, a rise in the yield of glutenin hydrolysates was observed, indicating a more solubilized mass over prolonged hydrolysis time. This trend is corroborated by the corresponding decrease in the average molecular weight of the hydrolysates, as shown in Table 1. The observed pattern suggests an increasing efficiency in the enzymatic treatment with extended hydrolysis times.

It is crucial to note the significant disparity in the hydrolytic

Table 2
The amino acid composition of the isolated glutenin fraction and its hydrolysates.

Amino acid	Content (mg/100 total protein mg, %)				
	Glutenin	Alc 5m	Alc 30m	Try 1h	Try 2h
Asp	4.4 ± 0.0	3.5 ± 0.0	2.9 ± 0.1	2.2 ± 0.2	2.6 ± 0.3
Glu	40.1 ± 0.0	68.7 ± 1.7	64.6 ± 3.8	66.7 ± 1.6	70.4 ± 3.4
Ser	6.0 ± 0.1	1.2 ± 0.1	0.7 ± 0.1	0.1 ± 0.1	0.1 ± 0.1
Thr	2.6 ± 0.0	1.5 ± 0.1	2.6 ± 1.0	4.1 ± 0.1	2.2 ± 0.2
Gly	5.2 ± 0.4	0.9 ± 0.1	1.0 ± 0.2	0.9 ± 0.1	0.8 ± 0.1
Ala	2.1 ± 0.1	4.6 ± 0.1	5.2 ± 0.3	4.2 ± 0.0	4.1 ± 0.1
Arg	6.5 ± 0.6	2.9 ± 0.2	3.5 ± 0.8	2.8 ± 0.2	2.4 ± 0.3
Pro	10.4 ± 0.5	5.7 ± 0.3	7.1 ± 0.4	6.7 ± 0.5	6.4 ± 0.7
Val	1.8 ± 0.7	0.0 ± 0.0	0.3 ± 0.0	0.2 ± 0.0	0.0 ± 0.0
Met	2.2 ± 0.5	2.0 ± 0.1	2.5 ± 0.6	2.4 ± 0.2	2.2 ± 0.4
Lle	5.5 ± 0.4	1.3 ± 0.1	1.4 ± 0.2	1.1 ± 0.0	0.7 ± 0.2
Leu	2.8 ± 0.2	1.1 ± 0.1	1.3 ± 0.3	1.3 ± 0.3	1.0 ± 0.2
Phe	1.1 ± 0.1	5.4 ± 0.6	5.8 ± 0.9	5.6 ± 0.2	5.4 ± 0.5
Cys	0.8 ± 0.0	0.2 ± 0.0	0.2 ± 0.0	0.3 ± 0.3	0.3 ± 0.0
Lys	2.0 ± 0.1	0.0 ± 0.0	0.0 ± 0.0	0.0 ± 0.0	0.0 ± 0.0
His	3.4 ± 0.1	0.0 ± 0.0	0.0 ± 0.0	0.1 ± 0.1	0.0 ± 0.0
Tyr	3.1 ± 0.3	1.0 ± 0.0	0.9 ± 0.3	0.8 ± 0.0	0.9 ± 0.1
Total protein content (mg protein/mg sample)	83.9 ± 5.3	96.5 ± 2.1	89.8 ± 1.1	100.1 ± 4.9	100.2 ± 1.3

capabilities of Alcalase and trypsin. The mass yield of Alcalase hydrolysates consistently exceeded 60 % within a short timeframe, typically less than half an hour. In contrast, trypsin hydrolysates, even with extended hydrolysis times of up to 4 h, only reached a maximum yield of 50 %. Additionally, there is a substantial difference in the average molecular weight, with Alcalase hydrolysates typically falling below 1 kDa, while trypsin hydrolysates tend to be around 10 kDa. This difference arises from the fact that trypsin only cleaves peptide bonds between Arg or Lys and the adjacent amino acid, while Alcalase works randomly on peptide bonds.

Despite all hydrolysates exhibiting weak IRI activity in the 1 x PBS solution compared to the negative polyethylene glycol (PEG) control, trypsin hydrolysates demonstrate significantly higher IRI activity compared to Alcalase hydrolysates. Specifically, the former inhibited the ice crystal size by approximately 30 %, while the latter showed less than a 20 % reduction, compared to negative control samples. It is significant, however, that previous studies on pig skin collagen, fish gelatin, and silver carp have consistently indicated that antifreeze peptides with molecular masses less than 3 kDa exhibited higher activity than those with molecular weights greater than 3 kDa (Chen, Wu, Cai, & Wang, 2021; Damodaran et al., 2017; Luo et al., 2023). It is important to recognize that these studies focused on animal-derived materials, while glutenin, being a plant protein, may exhibit different activity profiles. In addition, the profiles of peptides from different enzymes are distinct, which may contribute to the observed differences in activity.

3.2. Effect of amino acid profile on IRI activity

To analyze the effect of amino acid composition on IRI activity, four different glutenin hydrolysates generated with different enzymes and hydrolysis times (Try 1h, Try 2h, Alc 5m, and Alc 30m) were selected for further analysis. Table 2 displays the amino acid profile of these glutenin hydrolysates. Notably, Glu constitutes a significant portion, accounting for over 60 % of the total amino acids. Additionally, Pro content is substantial, ranking second. This difference in amino acid composition is an important factor that can influence the antifreeze activity of peptides (Chen et al., 2021).

The correlation between Glu and Pro with IRI activity is supported by previous studies. Polymers, composed of glutamic acids, such as oligo- and poly(glutamic acid)s, have demonstrated antifreeze activity (Mitsuiki, Mizuno, Tanimoto, & Motoki, 1998). Additionally, Wang et al. (2021) identified seven antifreeze peptides from silver carp sharing the same Glu-Glu sequences, proposing that this sequence might be linked to ice binding sites. Molecular simulations conducted by Luo et al. (2023) may provide further evidence, showing that Glu and Asp residues in peptides from silver carp can bind more free water, effectively inhibiting the formation and nucleation of ice crystals. Moreover, the presence of acidic amino acids, including Glu and Asp, introduces a negative charge in neutral conditions, and this negative charge has been linked to higher antifreeze activity (Yuan et al., 2023). Furthermore, proline has been previously linked to cryoprotective activity. L-proline, for example, has proven useful in the cryopreservation of cells (Liu et al., 2023). Peptides rich in proline, such as gelatin (Damodaran et al., 2017), or those containing Pro (Kim. et al., 2009), have demonstrated the ability to inhibit the growth of ice crystals. Studies by Rojas et al. (2022) also indicated that polyproline peptides exhibit higher thermal hysteresis activity compared to other homopeptides, such as Arg and Lys.

3.3. Effect of salt concentration in dispersing media on IRI activity

Fig. 1 shows that all four hydrolysates exhibit higher antifreeze activity at 0.1 x PBS than 1 x PBS. Notably, hydrolysates produced by trypsin consistently show superior activity compared to those generated by Alcalase at 0.1 x PBS. Specifically, the ice crystal size of Try 1h and Try 2h is too small to be analyzed by the automated images analysis program at the concentration of 40 mg/mL, and their ice crystal size relative to the same concentration of PEG (ICS %) values are 63.9 % and 70.9 %, respectively, even at a low concentration of 5 mg/mL. Additionally, the hydrolysate produced by Alcalase for 30 min exhibits significantly higher activity compared to the one produced for 5 min, particularly in the 0.1 x PBS solution. One interesting finding was the increase in hydrolysates' IRI activity as salt concentration decreased, observed in both PBS and NaCl solution. For example, ICS of Alcalase 5 min and Alcalase 30 min decreased by 26 % and 46 %, respectively, compared to the control. However, no significant difference in ice crystal size reduction is observed between the two trypsin samples, suggesting that salt concentration may have different impacts on glutenin peptides with different average molar masses.

The relationship between salt concentration and the IRI activity of antifreeze polymers is intricate and seemingly controversial. Various studies have illustrated a synergistic effect between salt concentration and IRI activity. For instance, Leiter et al. (2016) observed an enhancement in the activity of antifreeze protein III (AFP III) with the addition of 30 mM NaCl. Similarly, Hayakari and Hagiwara (2012) reported that the interaction between winter flounder antifreeze proteins and the ice surface was intensified by adding 147 mM NaCl. Conversely, Delesky (2020) found that the addition of 151 mM salts such as $CaCl_2$, $MgCl_2$, $CuCl_2$, or $AlCl_3$ reduced the IRI activity of poly (2-hydroxypropylmethacrylamide) and eliminated the IRI activity of polythreonine. However, the underlying mechanisms of these effects remain unexplored. Building on these observations, Wu et al. (2017). compared the impact of various salt solutions, without the presence of

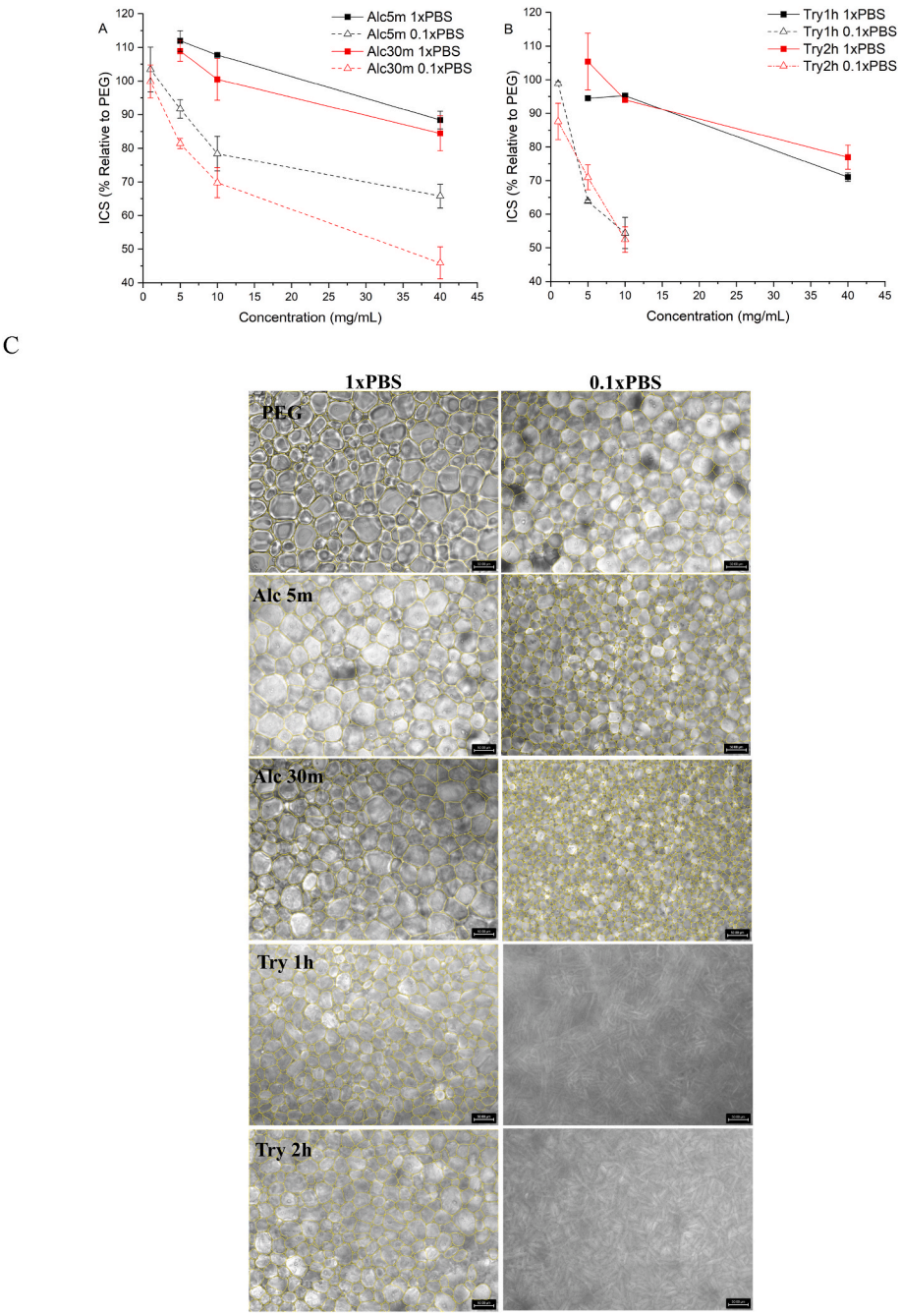

Fig. 1. Enzymatic hydrolysis and PBS concentration affected the IRI activity of wheat glutenin. A) IRI activity of Alcalase hydrolysates, B) IRI activity of trypsin hydrolysates, and C) representative ice images as affected by PBS concentration.

polymers, on the final crystal size at different salt concentrations. Their research showed the significant role of the Hofmeister series in final ice crystals size. Generally, the Hofmeister series seems to influence ice recrystallization, suggesting that the previous contradictory results may come from the differences in salt type. However, further research is needed to elucidate these interactions more clearly.

3.4. Effect of different cations on the IRI activity of wheat glutenin hydrolysates

In Fig. 2, the data for trypsin hydrolysates at 4 % were not included in the figure due to its unrecognizable small ice particles. Trypsin hydrolysates still displayed higher IRI activity than Alcalase hydrolysates in the $CaCl_2$ solution. In addition, all samples exhibited greater IRI activity in NaCl solutions compared to $CaCl_2$ solutions at the same concentration. However, the difference in antifreeze activity in trypsin hydrolysates was more pronounced than that in Alcalase hydrolysates.

It is important to note that the ionic strength of 10 mM NaCl and $CaCl_2$ solutions differs, and this variance in ionic strength could impact IRI activity. To ensure a fair comparison, we selected a 30 mM NaCl solution to equate the ionic strength of 10 mM $CaCl_2$. Interestingly, the ICS % of all hydrolysates is lower in the presence of Ca^{2+} at the same ionic strength (Fig. 2). Specifically, all four samples showed an ICS reduction of approximately 10 mM in $CaCl_2$ solution compared to NaCl solution at a concentration of 40 mg/mL, indicating that the type of cation also has an impact on IRI activity.

This suggests that Ca^{2+} can promote the IRI of glutenin hydrolysates compared to Na^{+}. A similar phenomenon was observed in Ca^{2+}

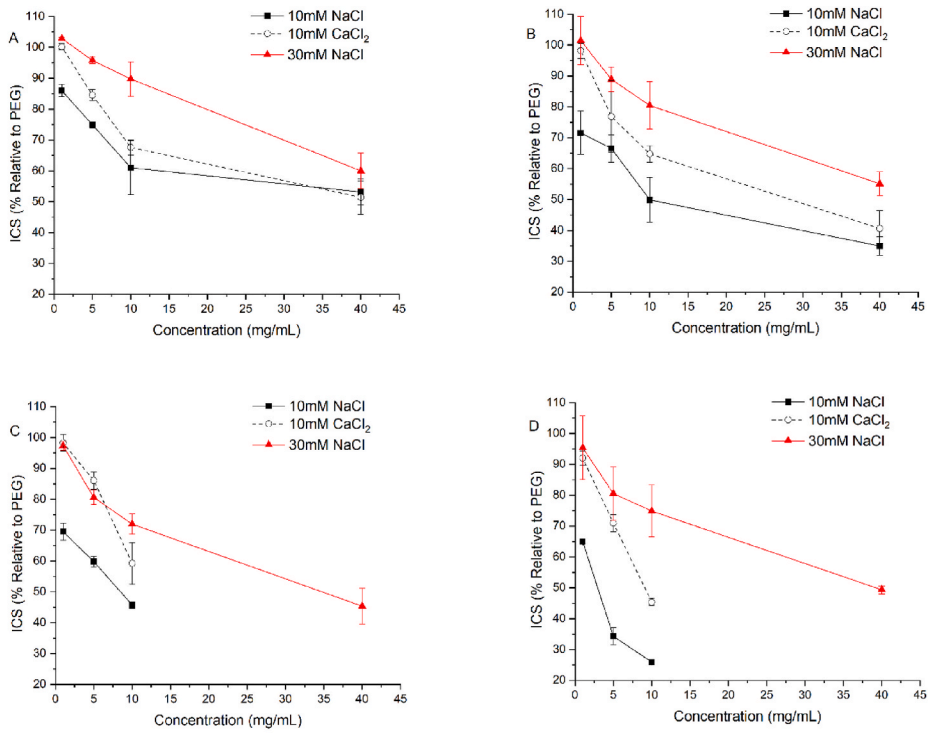

E

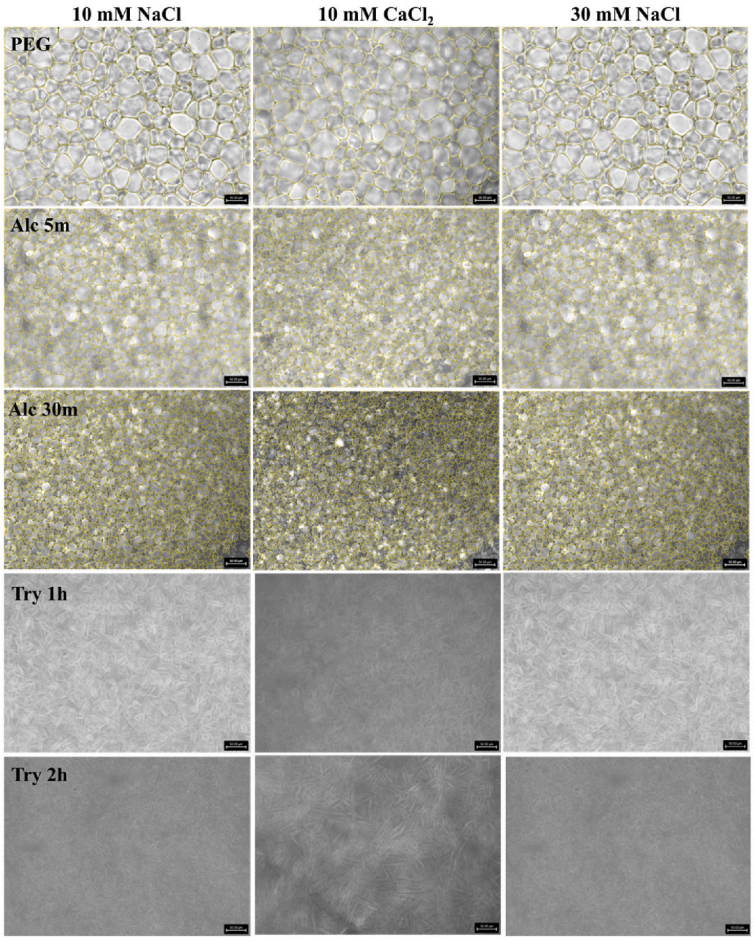

Fig. 2. Ionic strength and cation type affected the IRI activity of wheat glutenin hydrolysates (A: Alc 5m; B: Alc 30m; C: Try 1h; D: Try 2h, E: representative ice crystal images).

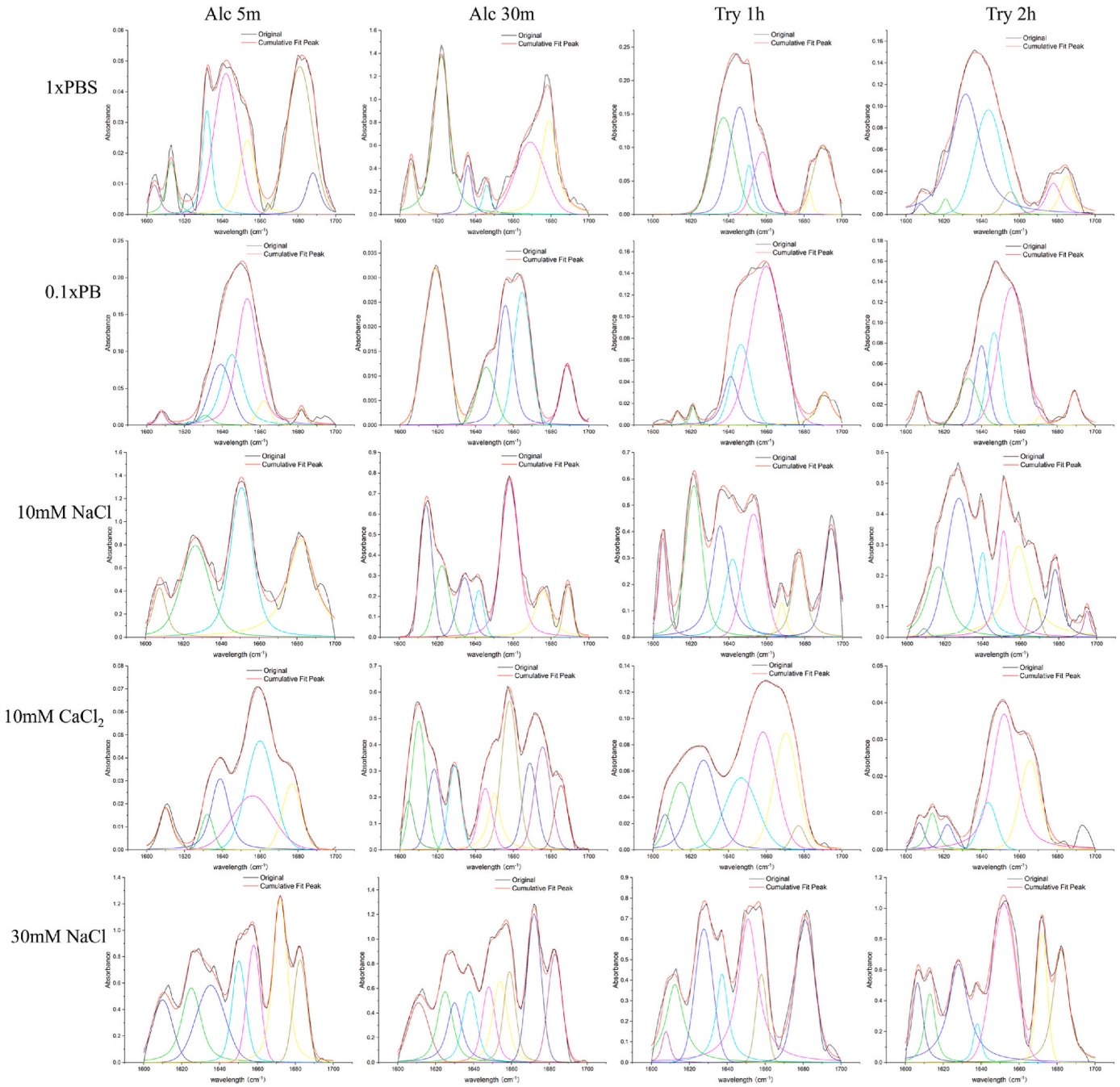

Fig. 3. The FTIR spectra of amide I band (1700-1600 cm^{-1}) of glutenin hydrolysates in different dispersing media at 40 mg/mL concentration and at room temperature.

dependent type II AFP, where Ca^{2+} binding residues are preferable to binding ice only in the Ca^{2+}-bound state. The presence of ice-like clathrate waters induced by Ca^{2+} binding facilitates the ice-binding capability of these proteins as well (Arai et al., 2019). This Ca^{2+} promoted IRI activity was also shared in other Ca^{2+} dependent antifreeze proteins (Vance et al., 2014) and certain lectins, such as soybean agglutinin, *R. communis* agglutinin, and human c-type lectins (Mitchell & Gibson, 2015). Despite being homologous to type II AFPs, these lectins does not possess inherent antifreeze activity. However, the existence of Ca^{2+} ions could effectively switch on and off their IRI activity. However, glutenin is neither a Ca^{2+} dependent protein nor homologous to type II AFPs, so the reason for this phenomenon remains unclear. Wu et al. (2017) suggested that high charge density ions preferentially reside at the ice-water interface, inhibiting ice growth, whereas ions with relatively low anions charge density do not. Although this observation was specifically related to anions, cations might follow a similar pattern. Given that Ca^{2+} has a higher charge density than Na^{+}, this characteristic could be a contributing factor to the superior IRI activity of wheat glutenin hydrolysates in 10 mM $CaCl_2$ dispersing media.

3.5. *Effect of dispersing medium on IRI of peptides*

The FT-IR spectrum in the 1600-1700 cm^{-1} regions is shown in Fig. 3, and Fig. 4 summarizes the secondary structure of hydrolysates in different dispersing media. Both figures showed that the salt concentration and types in the dispersing medium significantly influenced the secondary structure of peptides. Notably, a common trend across all hydrolysates was observed: lower salt concentrations (10–30 mM) led to

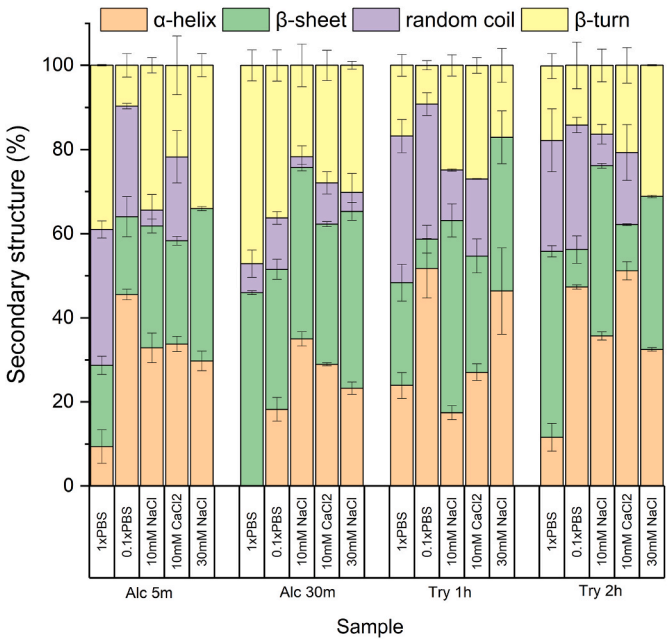

Fig. 4. The effect of dispersing media on secondary structure of glutenin hydrolysates.

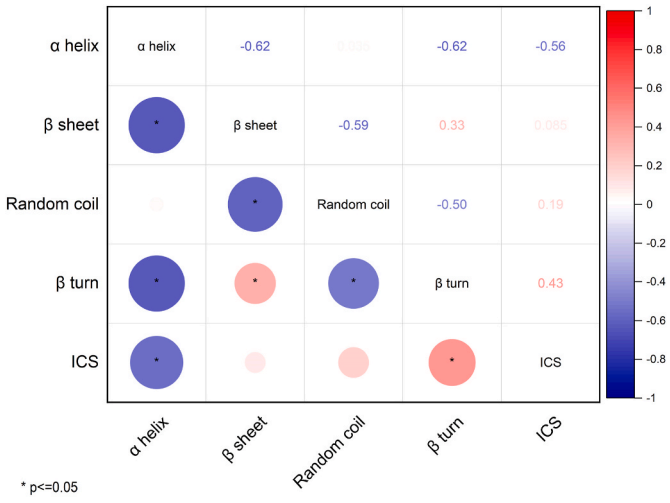

Fig. 5. Pearson's correlation coefficients for the secondary structure and IRI activity of glutenin hydrolysates in different dispersing media.

an increase in α-helix content and a decrease in β-turn content compared to the 1 x PBS solution with a concentration of about 150 mM. Furthermore, trypsin hydrolysates displayed a lower content of β-sheet structure in 0.1 x PBS than in 1 x PBS, whereas Alcalase hydrolysates did not exhibit this phenomenon. Additionally, the type of salt was found to impact the secondary structure. Under the same ionic strength, the content of α-helix in all four hydrolysates in a 10 mM $CaCl_2$ solution was higher than that in a 30 mM NaCl solution. In NaCl solutions, all hydrolysates tended to have minimal content of random coil, particularly in 30 mM NaCl. However, the secondary structure data for all samples in 10 mM $CaCl_2$ and NaCl solutions, on the other hand, were more like those in the 0.1 x PBS solution than the 1 x PBS solution. This suggests that salt concentration has a more significant influence than salt type on the conformation of peptides. Moreover, Fig. 4 also demonstrated that two trypsin hydrolysates exhibited a higher content of α-helix than Alcalase hydrolysates in 1 x PBS and 0.1 x PBS solutions. Considering the relationship between the structure rigidity and IRI activity, this higher

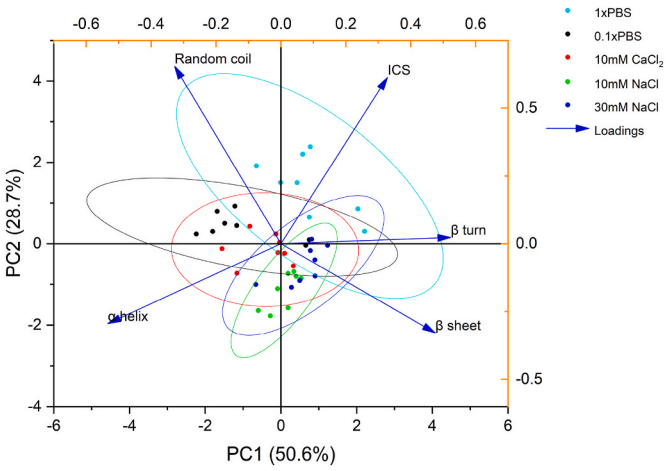

Fig. 6. Discriminant analysis of glutenin hydrolysates in various dispersing media (blue: 1 x PBS, black: 0.1 x PBS, green: 10 mM NaCl, red: 10 mM $CaCl_2$, and navy blue: 30 mM NaCl): a PCA-based classification model using scores plot and loading plots with 95% confidence ellipses.

content of α-helix may provide an explanation for the higher IRI activity of trypsin hydrolysates (Table 1).

From Fig. 5, a significant negative correlation ($P < 0.001$) is evident between the α-helix content and the ICS %, with an R value of −0.56. Conversely, there is a significant positive correlation ($P = 0.005$) between the β-turn content and the ICS %, with an R value of 0.43. These findings suggest that as the α-helix content increases and the β-turn content decreases, there is a corresponding increase in the IRI activity for glutenin hydrolysates. The rise in α-helix content and the decline in β-turn content typically signify an increase in structural rigidity, a characteristic associated with higher antifreeze activity (Patel et al., 2010). Because of this, the observed changes in conformation, especially the higher amount of α-helix in the dispersing media, may help explain the improvement in the IRI activity. Previous studies have shown that antifreeze peptides from different sources were characterized by α-helical structure (Shah et al., 2012; Wang et al., 2021; Yang et al., 2022; Zhu et al., 2022) which support our current observation on the effect of secondary structure on the IRI activity of wheat glutenin hydrolysates. We also observed a correlation between secondary structure and IRI activity, however a direct regulatory mechanism cannot be suggested. The extent to which this correlation applies to other IRI active proteins and peptides requires further investigation to elucidate underlying mechanisms.

3.6. The importance of dispersing medium on IRI activity of glutenin hydrolysates

To discern discrimination in various dispersing media, PCA and PLS-DA methods were employed. A total of 40 data sets obtained from four glutenin hydrolysates (Alc 5m, Alc 30m, Try 1h, and Try 2h) dispersed in five different media (1 x PBS, 0.1 x PBS, 10 mM NaCl, 10 mM $CaCl_2$, 30 mM NaCl) were analyzed. In the PCA model, the first principal component contributed 50.6 %, and the second principal component contributed 28.7 % of the variance. The PCA score plot aimed to demonstrate if the glutenin hydrolysates could be categorized based on different dispersing media. The greater the distance between groups, the more distinct the samples are. Fig. 6 displayed 95 % confidence ellipses overlapping with each cluster, indicating inadequate separation among groups, and suggesting that the PCA model did not effectively differentiate among the various dispersing media. However, it is noteworthy that the cluster of 1 x PBS exhibited relatively greater separation from the other groups, implying a more distinct profile in comparison. In addition, the direction of the arrows explained the correlation between

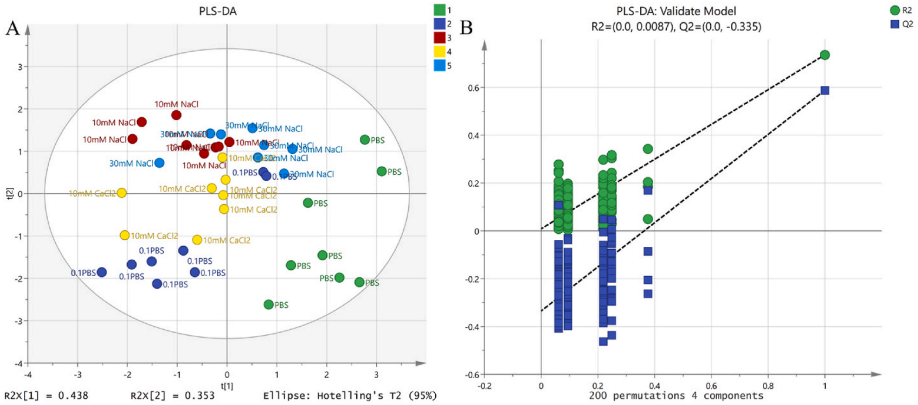

Fig. 7. Score plots (A), and 200 permutation tests (B) for the PLS-DA model of glutenin hydrolysates in different dispersing media.

the variables (Guo et al., 2023). Briefly, arrows pointing in the same direction indicate a positive correlation between the represented variables, while arrows pointing in opposite directions indicate a negative correlation. Among different secondary structures, there is an evident correlation between α-helix and antifreeze activity.

Fig. 7B was used to validate the PLS-DA model reliability. According to established conventions, modified R2 is not to exceed 0.3–0.4, and modified Q2 should be below 0.05, indicating the model does not suffer from overfitting (Eriksson, Byrne, Johansson, Trygg, & Vikström, 2013). However, adopting a more stringent criterion, all points on the left side should be below the right points, respectively, providing evidence of the model's reliability. The left data points represent Q_2 and R_2 values derived from 200 permutation tests, while the right two points illustrate Q_2 and R_2 values of the actual model (Eriksson et al., 2013; Li et al., 2018). In Fig. 7A, the PLS-DA plot illustrates a distinct separation between samples with 1 x PBS and those with lower concentration solutions. The solid points representing 1 x PBS are notably distant from other groups at low salt concentrations, underscoring the substantial influence of salt concentration compared to salt type. Furthermore, under similar salt concentrations, the position of the composite salt solution (0.1 x PBS) is slightly distant from the other three salt solutions with only one type of salt present. Samples in two different concentrations of NaCl solutions are closely grouped together, indicating that salt type still has an impact on the properties of gluten in hydrolysates, but this impact is less pronounced than the effect of salt concentration.

4. Conclusion

In summary, wheat glutenin hydrolysates, generated using Alcalase and trypsin, exhibited modest IRI activity in a 1 x PBS solution, potentially linked to their high content of Glu and Pro. Notably, trypsin-derived hydrolysates consistently demonstrated superior antifreeze properties compared to those produced by Alcalase in different dispersing media, and these differences may stem from variations in molecular mass or peptide residues. One interesting finding was the increase in hydrolysates' IRI activity as salt concentration decreased, observed in both PBS and NaCl solution. Additionally, all hydrolysates showed higher IRI activity in $CaCl_2$ solution than in NaCl solution, under the same ionic strength, indicating that the type of cation also has an impact on IRI activity. However, salt concentration appears to have a more significant impact than salt type on IRI activity. The observed improvement in activity in different solutions correlated with changes in secondary structure, characterized by increased α-helix content and reduced β-turns. These findings suggest that the observed improvement in IRI activity for glutenin hydrolysates is associated with increased structural rigidity. We observed that both the secondary structure of wheat glutenin hydrolysates and the salt concentration in the dispersing medium used in the splat assay contribute to the IRI activity.

CRediT authorship contribution statement

Yuan Yuan: Writing – original draft, Visualization, Validation, Methodology, Investigation, Formal analysis, Data curation, Conceptualization. **Vermont P. Dia:** Writing – review & editing, Resources, Project administration, Funding acquisition, Conceptualization. **Tong Wang:** Writing – review & editing, Resources, Project administration, Funding acquisition, Data curation, Conceptualization.

Declaration of Competing interest

The authors declare that they have no conflict of interests.

Data availability

Data will be made available on request.

Acknowledgements

This study was supported by the National Science Foundation through funding (award number 2103558).

References

Akhlaghi, Y., Ghaffari, S., Attar, H., & Alamir Hoor, A. (2015). A rapid hydrolysis method and DABS-Cl derivatization for complete amino acid analysis of octreotide acetate by reversed phase HPLC. *Amino Acids, 47*(11), 2255–2263. https://doi.org/10.1007/s00726-015-1999-9

Arai, T., Nishimiya, Y., Ohyama, Y., Kondo, H., & Tsuda, S. (2019). Calcium-binding generates the semi-clathrate waters on a type II antifreeze protein to adsorb onto an ice crystal surface. *Biomolecules, 9*(5). https://doi.org/10.3390/biom9050162

Bachtiger, F., Congdon, T. R., Stubbs, C., Gibson, M. I., & Sosso, G. C. (2021). The atomistic details of the ice recrystallisation inhibition activity of PVA. *Nature Communications, 12*(1), 1323. https://doi.org/10.1038/s41467-021-21717-z

Biggs, C., Stubbs, C., Graham, B., Fayter, A. E. R., Hasan, M., & Gibson, M. I. (2019). Mimicking the ice recrystallization activity of biological antifreezes. when is a new polymer "active". *Macromolecular Bioscience, 19*(7), Article e1900082. https://doi.org/10.1002/mabi.201900082

Chen, X., Wu, J., Cai, X., & Wang, S. (2021). Production, structure-function relationships, mechanisms, and applications of antifreeze peptides. *Comprehensive Reviews in Food Science and Food Safety, 20*(1), 542–562. https://doi.org/10.1111/1541-4337.12655

Damodaran, S., & Wang, S. (2017). Ice crystal growth inhibition by peptides from fish gelatin hydrolysate. *Food Hydrocolloids, 70*, 46–56. https://doi.org/10.1016/j.foodhyd.2017.03.029

Delesky, E. A. (2020). *Ice recrystallization inhibition of ice-binding proteins and bioinspired synthetic mimics in non-physiological environments*. University of Colorado at Boulder.

Delesky, E. A., & Srubar, W. V. (2022). Ice-binding proteins and bioinspired synthetic mimics in non-physiological environments. *iScience, 25*(5), Article 104286. https://doi.org/10.1016/j.isci.2022.104286

Eriksson, L., Byrne, T., Johansson, E., Trygg, J., & Vikström, C. (2013). *Multi-and megavariate data analysis basic principles and applications: Umetrics Academy*.

Guo, H., Zheng, Y.-J., Wu, D.-T., Du, X., Gao, H., Ayyash, M., … Gan, R.-Y. (2023). Quality evaluation of citrus varieties based on phytochemical profiles and nutritional properties. *Frontiers in Nutrition, 10*, Article 1165841.

Hayakari, K., & Hagiwara, Y. (2012). Effects of ions on winter flounder antifreeze protein and water molecules near an ice/water interface. *Molecular Simulation, 38*(1), 26–37.

Kim, J. S., Damodaran, S., & Yethiraj, A. (2009). Retardation of ice crystallization by short peptides. *J. Phys. Chem., A*(113), 4403–4407.
Knight, C. A., Hallett, J., & DeVries, A. (1988). Solute effects on ice recrystallization: An assessment technique. *Cryobiology, 25*(1), 55–60.
Leiter, A., Rau, S., Winger, S., Muhle-Goll, C., Luy, B., & Gaukel, V. (2016). Influence of heating temperature, pressure and pH on recrystallization inhibition activity of antifreeze protein type III. *Journal of Food Engineering, 187*, 53–61. https://doi.org/10.1016/j.jfoodeng.2016.04.019
Li, Y., Wang, D., Zeng, C., Liu, Y., Huang, G., & Mei, Z. (2018). Salivary metabolomics profile of patients with recurrent aphthous ulcer as revealed by liquid chromatography–tandem mass spectrometry. *Journal of International Medical Research, 46*(3), 1052–1062. https://doi.org/10.1177/0300060517745388
Liu, C., Feng, H., Han, J., Zhou, H., Yuan, L., Pan, H., … Li, X. (2023). Effect of L-proline on sperm quality during cryopreservation of boar semen. *Animal Reproduction Science, 258*, Article 107359. https://doi.org/10.1016/j.anireprosci.2023.107359
Lookhart, G. E. O. R., & Scott, B. (1995). Separation and characterization of wheat protein fractions by high-performance capillary electrophoresis. *Cereal Chemistry, 72*(6), 527–532.
Luo, W., Yuan, C., Wu, J., Liu, Y., Wang, F., Li, X., et al. (2023). Inhibition mechanism of membrane-separated silver carp hydrolysates on ice crystal growth obtained through experiments and molecular dynamics simulation. *Food Chemistry, 414*, Article 135695. https://doi.org/10.1016/j.foodchem.2023.135695
Mitchell, D. E., Clarkson, G., Fox, D. J., Vipond, R. A., Scott, P., & Gibson, M. I. (2017). Antifreeze protein mimetic metallohelices with potent ice recrystallization inhibition activity. *J Am Chem Soc, 139*(29), 9835–9838. https://doi.org/10.1021/jacs.7b05822
Mitchell, D. E., & Gibson, M. I. (2015). Latent ice recrystallization inhibition activity in nonantifreeze proteins: Ca2+-activated plant lectins and cation-activated antimicrobial peptides. *Biomacromolecules, 16*(10), 3411–3416. https://doi.org/10.1021/acs.biomac.5b01118
Mitsuiki, M., Mizuno, A., Tanimoto, H., & Motoki, M. (1998). Relationship between the antifreeze activities and the chemical structures of oligo- and poly(glutamic acid)s. *Journal of Agricultural and Food Chemistry, 46*(3), 891–895. https://doi.org/10.1021/jf970797m
Mochizuki, K., & Molinero, V. (2018). Antifreeze glycoproteins bind reversibly to ice via hydrophobic groups. *J Am Chem Soc, 140*(14), 4803–4811. https://doi.org/10.1021/jacs.7b13630
Nielsen, S. S. (2017). *Food analysis laboratory manual*. Springer.
Nishimiya, Y., Kondo, H., Yasui, M., Sugimoto, H., Noro, N., Sato, R., … Tsuda, S. (2006). Crystallization and preliminary X-ray crystallographic analysis of Ca2+-independent and Ca2+-dependent species of the type II antifreeze protein. *Acta Crystallographica, Section F: Structural Biology and Crystallization Communications, 62*(6), 538–541.
Patel, S. N., & Graether, S. P. (2010). Increased flexibility decreases antifreeze protein activity. *Protein Science, 19*(12), 2356–2365. https://doi.org/10.1002/pro.516
Rojas, R., Aróstica, M., Carvajal-Rondanelli, P., Albericio, F., Guzmán, F., & Cárdenas, C. (2022). Relationship between type II polyproline helix secondary structure and thermal hysteresis activity of short homopeptides. *Electronic Journal of Biotechnology, 59*, 62–73. https://doi.org/10.1016/j.ejbt.2022.08.003
Saad, J., Fomich, M., Dia, V. P., & Wang, T. (2023). Anovel automated protocol for ice crystal segmentation analysis using Cellpose and Fiji. *Journal of Cryobiology, 111*, 1–8.
Sadat, A., Corradini, M. G., & Joye, I. J. (2019). Molecular spectroscopy to assess protein structures within cereal systems. *Current Opinion in Food Science, 25*, 42–51. https://doi.org/10.1016/j.cofs.2019.02.001
Sadat, A., & Joye, I. J. (2020). Peak fitting applied to fourier transform infrared and Raman spectroscopic analysis of proteins. *Applied Sciences, 10*(17). https://doi.org/10.3390/app10175918
Shah, S. H., Kar, R. K., Asmawi, A. A., Rahman, M. B., Murad, A. M., Mahadi, N. M., … Bhunia, A. (2012). Solution structures, dynamics, and ice growth inhibitory activity of peptide fragments derived from an antarctic yeast protein. *PLoS One, 7*(11), Article e49788. https://doi.org/10.1371/journal.pone.0049788
Sicheri, F., & Yang, D. (1996). Structure determination of a lone α-helical antifreeze protein from winter flounder. *Acta Crystallographica Section D: Biological Crystallography, 52*(3), 486–498.
Sivam, A. S., Sun-Waterhouse, D., Quek, S., & Perera, C. O. (2010). Properties of bread dough with added fiber polysaccharides and phenolic antioxidants: A review. *Journal of Food Science, 75*(8), R163–R174. https://doi.org/10.1111/j.1750-3841.2010.01815.x
Spellman, D., McEvoy, E., O'Cuinn, G., & FitzGerald, R. J. (2003). Proteinase and exopeptidase hydrolysis of whey protein: Comparison of the TNBS, OPA and pH stat methods for quantification of degree of hydrolysis. *International Dairy Journal, 13*(6), 447–453. https://doi.org/10.1016/s0958-6946(03)00053-0
Suris-Valls, R., & Voets, I. K. (2019). The impact of salts on the ice recrystallization inhibition activity of antifreeze (glyco)proteins. *Biomolecules, 9*(8). https://doi.org/10.3390/biom9080347
Thewissen, B. G., Celus, I., Brijs, K., & Delcour, J. A. (2011). Foaming properties of wheat gliadin. *Journal of Agricultural and Food Chemistry, 59*(4), 1370–1375. https://doi.org/10.1021/jf103473d
Tsumoto, K., Ejima, D., Senczuk, A. M., Kita, Y., & Arakawa, T. (2007). Effects of salts on protein-surface interactions: Applications for column chromatography. *J Pharm Sci, 96*(7), 1677–1690. https://doi.org/10.1002/jps.20821
Urade, R., Sato, N., & Sugiyama, M. (2018). Gliadins from wheat grain: An overview, from primary structure to nanostructures of aggregates. *Biophys Rev, 10*(2), 435–443. https://doi.org/10.1007/s12551-017-0367-2
Vance, T. D., Olijve, L. L., Campbell, R. L., Voets, I. K., Davies, P. L., & Guo, S. (2014). Ca2+-stabilized adhesin helps an Antarctic bacterium reach out and bind ice. *Bioscience Reports, 34*(4). https://doi.org/10.1042/bsr20140083
Voets, I. K. (2017). From ice-binding proteins to bio-inspired antifreeze materials. *Soft Matter, 13*(28), 4808–4823. https://doi.org/10.1039/c6sm02867e
Wang, F., Cui, M., Liu, H., Li, X., Yu, J., Huang, Y., et al. (2021). Characterization and identification of a fraction from silver carp (Hypophthalmichthys molitrix) muscle hydrolysates with cryoprotective effects on yeast. *LWT, 137*. https://doi.org/10.1016/j.lwt.2020.110388
Wieser, H., Koehler, P., & Scherf, K. A. (2022). Chemistry of wheat gluten proteins: Quantitative composition. *Cereal Chemistry, 100*(1), 36–55. https://doi.org/10.1002/cche.10553
Wu, S., Zhu, C., He, Z., Xue, H., Fan, Q., Song, Y., et al. (2017). Ion-specific ice recrystallization provides a facile approach for the fabrication of porous materials. *Nature Communications, 8*, Article 15154. https://doi.org/10.1038/ncomms15154
Yang, F., Jiang, W., Chen, X., Chen, X., Wu, J., Huang, J., … Wang, S. (2022). Identification of novel antifreeze peptides from takifugu obscurus skin and molecular mechanism in inhibiting ice crystal growth. *Journal of Agricultural and Food Chemistry, 70*(44), 14148–14156. https://doi.org/10.1021/acs.jafc.2c04393
Yuan, Y., Fomich, M., Dia, V. P., & Wang, T. (2023). Succinylation of zein and gelatin hydrolysates improved their ice recrystallization inhibition activity. *Food Chemistry, 424*, Article 136431. https://doi.org/10.1016/j.foodchem.2023.136431
Zhang, Y., Liu, K., Li, K., Gutowski, V., Yin, Y., & Wang, J. (2018). Fabrication of anti-icing surfaces by short alpha-helical peptides. *ACS Appl Mater Interfaces, 10*(2), 1957–1962. https://doi.org/10.1021/acsami.7b13130
Zhang, Y., Wang, W., Liu, Y., Liu, X., Wang, H., & Zhang, H. (2022). Cryoprotective effect of wheat gluten enzymatic hydrolysate on fermentation properties of frozen dough. *Journal of Cereal Science, 104*. https://doi.org/10.1016/j.jcs.2022.103423
Zhu, K., Zheng, Z., & Dai, Z. (2022). Identification of antifreeze peptides in shrimp byproducts autolysate using peptidomics and bioinformatics. *Food Chemistry, 383*, Article 132568. https://doi.org/10.1016/j.foodchem.2022.132568